Journal of Molecular Science

Journal of Molecular Science
Volume 36 Issue 2, Year of Publication 2026, Page 431-445
DoI-10.004687/1000-9035.2026.053

Journal of Molecular Science
www.jmolecularsci.com ISSN:1000-9035

Development and Optimization of Tazarotene Loaded Glycerosome: A Novel Approach to Minimize Irritation in Acne Management

Sanjyot S. Taware[1], Kiran K. Shinde[2], Yogesh B. Tambade[3]

[1]Student, Department of Pharmaceutical Quality Assurance, Vidya Niketan Institute of Pharmacy and Research center Bota, Tal-Sangamner, Dist-A. Nagar, Pin Code- 422602.

[2]Associate Professor, Department of Pharmaceutical Quality Assurance,Vidya Niketan Institute of Pharmacy and Research center Bota, Tal-Sangamner, Dist-A. Nagar, Pin Code- 422602.

[3]Assistant Professor, Department of Pharmaceutical Quality Assurance, Vidya Niketan Institute of Pharmacy and Research center Bota, Tal-Sangamner, Dist-A. Nagar, Pin Code- 422602.

Article Information
Received: 24-04-2026
Revised: 17-05-2026
Accepted: 02-06-2026
Published: 26-06-2026

Keywords
Tazarotene; Glycerosomes; Box-Behnken Design; Topical Drug Delivery; Acne; Vesicular System; Thin Film Hydration.

ABSTRACT

Objectives: Tazarotene, a third-generation synthetic retinoid, routinely induces cutaneous irritation upon topical application, substantially narrowing its clinical applicability in acne vulgaris management. This work aimed to construct and statistically refine tazarotene-loaded glycerosomes as a nanovesicular phospholipid platform to enhance dermal permeation, sustain controlled drug release, and reduce local intolerance. **Methods:** Nanovesicles were fabricated by lipid film hydration and optimized via a three-factor, three-level Box-Behnken experimental design, employing phosphatidylcholine content, glycerol proportion, and Tween 80 level as independent input variables, with vesicular diameter and encapsulation efficiency as the quantified response outputs. The optimized glycerosomal dispersion was subsequently incorporated into a Carbopol 934-based hydrogel and comprehensively appraised for physicochemical characteristics, membrane-based drug permeation behavior, and accelerated stability in compliance with ICH Q1A(R2) guidelines. **Results:** Both regression models exhibited outstanding predictive fitness, achieving adjusted R^2 values of 0.9996 and 0.9970, respectively. Desirability-optimized batch F4 (desirability index: 1.0) attained a vesicular diameter of 152.4 ± 1.5 nm, PDI of 0.176 ± 0.007, surface charge of −24.7 ± 1.3 mV, and encapsulation efficiency of 90.9 ± 0.4%. Glycerosomal gel GG3 demonstrated viscosity of 4632 ± 31.2 cP, spreadability of 16.74 ± 0.31 g·cm/s, cumulative permeation of 67.4 ± 0.6% across 12 hours, and retained full physicochemical integrity without meaningful attribute deviation throughout three months of accelerated storage. **Conclusion:** The tazarotene glycerosomal gel system constitutes a scientifically grounded and therapeutically compelling dermal platform uniting controlled drug exposure with substantially reduced skin reactivity, warranting rigorous in vivo and clinical evaluation for its definitive translation into acne therapy.

1. INTRODUCTION:

Acne vulgaris is a skin inflammation that is one of the most common chronic inflammatory skin diseases in the world, having a prevalence of 9.4% of the worldwide population, and it is the eighth most common disease worldwide [1]. It primarily affects adolescents and young adults aged 12–25 years although the uptake among adults has increased significantly in the past few decades [2]. Many pathological mechanisms are involved such as hyperactivity of sebaceous glands, abnormal keratinization of the follicles, colonization by

Journal of Molecular Science
Volume 36 Issue 2, Year of Publication 2026, Page 431-445
DoI-10.004687/1000-9035.2026.053

Cutibacterium acnes and inflammatory cascades [3]. In addition to its physical manifestations, acne brings with it a heavy psychosocial burden and can lead to anxiety, depression and poor self-esteeam and quality of life in affected people. From an economic perspective, the cost of acne-related health care exceeds billions of dollars per year, including the cost of prescription medications, over-the-counter remedies and dermatological visits [4]. Retinoids, antibiotics and benzoyl peroxide are well-established topical treatments that often suffer from side effects of skin irritation, resistance to the antibiotic treatment, poor patient adherence and less than optimal penetration of the stratum corneum. In conclusion, the challenges faced with acne that persist highlight the critical need for the development of new, patient-friendly therapeutic strategies to address this issue [5].

Tazarotene is a third generation acetylenic retinoid that has proven to be a pharmacologically potent drug in the treatment of acne based on its very selective mode of action. It is chemically a prodrug, which is fast hydrolyzed into its active metabolite tazarotenic acid to which the RARβ and RARγ receptors in the skin bind selectively [6]. This receptor-selective binding affects the expression of genes involved in the abnormal proliferation of keratinocytes, their differentiation and hyperkeratinisation, all of which are key steps in the development of acne [7]. Moreover, the anti-inflammatory activity of tazarotene is shown by its ability to inhibit pro-inflammatory mediators in the pilosebaceous unit, which is the area where comedones form [8]. Even though it has been clinically proven to be an effective therapeutic agent, clinical use of tazarotene has been severely limited by its high cutaneous irritation profile, characterized by erythema, dryness, peeling, and a burning sensation, especially at higher concentrations. Such side effects significantly affect patient compliance and quality of therapy [9]. Therefore, research and development of an optimized delivery system which would permit the sustained therapeutic potential of tazarotene while reducing its irritation profile is a very attractive and clinically relevant goal [10].

Glycerosomes are a new generation of ultra deformable phospholipid-based vesicular carrier systems with a high amount of glycerol (hydrophobic component) in the bilayer structure generally 20-30% w/v of the total carrier volume [11]. Glycerosomes prove to have highly superior skin permeation properties, which are due to the hygroscopic nature of glycerol that keeps the membrane fluidity, decreases the rigidity of the membrane and allows to make efficient transdermal drug transport without disturbing the structure of the stratum corneum [12]. The glycerol also provides the formulation with significant moisturizing and emollient effects, which work against the often required extra moisturizing effect that retinoid therapy alone can cause [13]. In recent years, vesicles have consistently been shown to provide highly penetrating and controlled drug release from topical formulations and to retain a drug in specific layers of the skin versus traditional topical formulations [14]. Furthermore, the biocompatibility and biodegradability of the glycerosomes are attractive properties, especially for chronic dermatological uses. Additionally, their ability to form complexes with hydrophobic drugs, including tazarotene, with high entrapment efficiency, supports their use as an optimal delivery vehicle in this study [15].

This present study is directed towards the development, optimization and characterization of tazarotene loaded glycerosomes as a novel topical topical delivery system in the management of acne. Specific objectives comprise optimization of formulation variables using experimental design, physicochemical characterization, in vitro drug release/permeation studies and ex vivo skin deposition studies. The study also aims to demonstrate the superiority in safety and tolerability of the formulated product over standard tazarotene products.

MATERIALS AND METHODS:

MATERIALS:

Tazarotene, serving as the active pharmaceutical ingredient, was secured at API grade with a certified purity of not less than 99%, supplied by Research Lab Fine Chem Industries, Mumbai, India. The same commercial source furnished all formulation-grade excipients phosphatidylcholine, cholesterol, glycerol, polysorbate 80, Carbopol 934, methylparaben, propylene glycol, and triethanolamine each conforming to analytical grade standards. Solvents integral to both formulation and analytical procedures, namely methanol, ethanol, acetone, and chloroform, were of HPLC purity; potassium bromide was of spectroscopic grade; and phosphate buffer salts were analytically pure all drawn from the same commercial house. Any additional chemicals and reagents incorporated at various stages of the investigation satisfied analytical grade criteria and were employed directly, without subjecting them to any supplementary purification step before use.

METHODS:

Calibration Curve Determination of Tazarotene:
A stock solution of Tazarotene (1000 µg/mL in HPLC-grade methanol) was prepared and an aliquot of 0.5–3.0 mL was transferred to each of separate 100 mL volumetric flasks and made to mark with the

Journal of Molecular Science
Volume 36 Issue 2, Year of Publication 2026, Page 431-445
DoI-10.004687/1000-9035.2026.053

phosphate buffer pH 7.4, resulting in working concentrations of 5-30 µg/mL. Each one of the solutions was scanned in the UV-Visible spectrophotometer (Systronics, Model UV-2202, India) using quartz cuvettes (path length 1 cm) at its λ_{max}, with phosphate buffer at pH 7.4 used as blank, at 25° ± 0.5°C. After calibration, the graph of absorbance versus concentration (µg/ml) was plotted and thereafter, linearity was assessed by linear regression ($y = mx + c$), where $r^2 \geq 0.999$ was considered acceptable based on ICH Q2(R1) guidelines [16].

Solubility Study of Tazarotene

Equilibrium saturation solubility of tazarotene was assessed across eight physicochemically distinct media distilled water, phosphate buffer at pH 5.5, phosphate buffer at pH 7.4, methanol, ethanol, acetone, chloroform, and glycerol. Individual 5 mL volumes of each medium were transferred into sealed glass vessels, into which tazarotene was introduced at a loading concentration of 1.5 mol dm^{-3}. Each vessel was agitated continuously in a motorized mechanical shaker (Remi, Model CIS-24 Plus, India) at 25 ± 1°C for 24 hours until equilibrium saturation was achieved. The undissolved drug fraction was subsequently pelleted by centrifugation at 3000 rpm for 10 minutes, and the clarified supernatant was recovered by passage through Whatman No. 41 grade filter paper. Each filtrate was diluted with its corresponding medium to bring the drug concentration within the validated linear detection range. Tazarotene content was then quantified by UV spectrophotometry at the pre-established λmax, with concentrations derived by interpolation from a pre-validated calibration function. Solubility values were expressed in mg/mL. All determinations were performed in triplicate (n = 3), with results recorded as mean ± SD [17].

Differential Scanning Calorimetry:

To probe the thermophysical properties of tazarotene and screen for molecular-level interactions with proposed formulation excipients, calorimetric analysis was conducted on a TA Instruments DSC (Model Q200, USA). Accurately weighed quantities of neat tazarotene and its binary physical admixtures with individual excipients, in the 3 to 5 mg range, were hermetically crimped into standard aluminum crucibles; an identically prepared, unfilled crucible served as the thermal reference throughout each run. Under a continuous nitrogen blanket at a regulated flow of 50 mL/min, each sample underwent a linear temperature ramp of 10°C/min, scanning from 30°C to an upper boundary of 300°C. The resulting thermograms were interrogated for any shift, suppression, or emergence of heat flow events, with attention to transition onset temperatures, peak maxima, and associated enthalpy values. All calorimetric runs were executed in triplicate (n = 3), and data are reported as mean ± SD [18,19].

Fourier Transform Infrared Spectroscopy:

The functional groups of Tazarotene were identified by Fourier Transform Infrared (FTIR) spectroscopy and drug-excipient compatibility was assessed by an FTIR spectrophotometer (Model: Alpha, Bruker, Germany). KBr pellet method of spectra recording was used here for pure Tazarotene and physical mixture of Tazarotene and excipients ratio (1:100), and the resulting pellets were compressed with hydraulic pressure to get a transparent pellet. The pellets were scanned and absorption peaks were recorded and interpreted between 4000 cm^{-1} to 400 cm^{-1} at 4cm^{-1} resolution to identify specific functional groups. The assays were carried out in triplicate (n = 3) [20,21].

Experimental Design for Optimization of Tazarotene-Loaded Glycerosomes:

The effect of independent variables on selected responses in the glycerosome formulation optimization was evaluated by a three-factor, three-level Box-Behnken design (BBD) designed using Design-Expert® software (Version 13, Stat-Ease Inc., Minneapolis, USA). The independent variables were selected for further study and include phosphatidylcholine concentration (X_1), glycerol concentration (X_2) and concentration of Tween 80 (X_3) at three levels, low (−1), medium (0), and high (+1), as shown in Table 1. Vesicle size (Y_1, to minimize) and encapsulation efficiency (Y_2, to maximize) were selected as dependent variables. The design produced 17 experimental runs with five center runs to estimate experimental error and the repeatability [22,23].

Table 1: Independent Variables with Levels and Dependent Variables with Goals

Independent Variable	Low (-1)	Medium (0)	High (+1)
Phosphatidyl choline (mg)	200	300	400
Glycerol (%)	20	30	40
Tween 80 (%)	1	1.5	2
Dependent Variables			**Goals**
Vesicle size (nm)			Minimize
Encapsulation efficiency (% EE)			Maximize

Formulation of Tazarotene-Loaded Glycerosomes:

The thin film hydration method was used to prepare tazarotene loaded glycerosomes. Phosphatidylcholine (200-400 mg as per experimental design) and cholesterol (10% w/w of phosphatidylcholine) were dissolved in a round-bottom flask containing chloroform:methanol (2:1 v/v) with labelled quantity of Tazarotene (10 mg). The organic solvent was completely dried by a

Journal of Molecular Science
Volume 36 Issue 2, Year of Publication 2026, Page 431-445
DoI-10.004687/1000-9035.2026.053

rotary evaporator (Heidolph, Model Laborota 4000, Germany) at 40°C, under reduced pressure (60 rpm) to deposit a thin uniform lipid film on the inner wall of the flask. The film was further dried for 30 minutes by purging with nitrogen gas to remove the remaining solvent. The amount of drying of lipid film, the amount of aqueous phase (glycerol 20, 30 or 40% v/v and Tween 80 1, 1.5 or 2% v/v) and the duration of the hydration process (60 minutes) at 60°C with constant rotation were within the range of experimental design. This vesicular dispersion was probe sonicated (Sonics, Vibra-Cell, USA) for 3 minutes in pulse mode (10 s on and 5 s off) in an ice bath to get a homogeneous dispersion of vesicles and reduce their size. A Box-Behnken design was used for seventeen formulation batches (F1–F17) prepared as outlined in Table 2 [24,25].

Table 2: Box-Behnken Design Layout for Tazarotene-loaded Glycerosome Formulation Batches

Batch	Tazarotene (mg)	Phosphatidylcholine (mg)	Glycerol (%)	Tween 80 (%)
F1	10	400	30	1
F2	10	200	40	1.5
F3	10	200	30	1
F4	10	300	40	2
F5	10	300	30	1.5
F6	10	300	20	1
F7	10	200	20	1.5
F8	10	400	20	1.5
F9	10	400	40	1.5
F10	10	300	30	1.5
F11	10	200	30	2
F12	10	300	30	1.5
F13	10	400	30	2
F14	10	300	40	1
F15	10	300	30	1.5
F16	10	300	20	2
F17	10	300	30	1.5

Formulation of Glycerosomal Gel:

A tazarotene-loaded glycerosomal dispersion was formulated into gel as a suitable topical formulation using Carbopol 934. Four batches of gel were formulated by varying the concentration of Carbopol 934 (0.5, 0.75, 1.0 and 1.25w/w) keeping all other ingredients constant as shown in Table 3. The necessary amount of Carbopol 934 was carefully weighed for each batch, slowly dispersed in purified water sufficient to completely cover it, and then left to swell for 24 hours with constant magnetic stirring at room temperature. Under constant stirring, the Carbopol dispersion was mixed with 0.1% w/w of methylparaben which was dissolved by gently warming it in 5% w/w propylene glycol. The glycerosomal dispersion (0.1 % w/w Tazarotene) was then gradually added to the formulation with slow stirring to prevent foaming and the damage of the vesicles. Carbopol was neutralized by dropwise addition of triethanolamine (TEA) while constantly stirring to get a clear, smooth and homogeneous gel with pH 6.0–6.5. For each batch 100 g was made up to with purified water and stored in closed containers at room temperature until further assessment [24,25].

Table 3: Formulation Composition of Tazarotene Glycerosomal Gel Batches

Ingredient	GG1	GG2	GG3	GG4
Glycerosomes (equiv. to Tazarotene)	0.1% w/w	0.1% w/w	0.1% w/w	0.1% w/w
Carbopol 934	0.5 g	0.75 g	1.0 g	1.25 g
Triethanolamine (TEA)	q.s.	q.s.	q.s.	q.s.
Propylene Glycol	5.0 g	5.0 g	5.0 g	5.0 g
Methylparaben	0.1 g	0.1 g	0.1 g	0.1 g
Purified Water	q.s. to 100 g	q.s. to 100 g	q.s. to 100 g	q.s. to 100 g

Characterization of tazarotene loaded glycerosomes:

Vesicle Size and Polydispersity Index (PDI):

The size and polydispersity index (PDI) of all seventeen batches of glycerosome formulations (F1 – F17) were measured using dynamic light scattering (DLS) with Malvern Zetasizer Nano ZS (Malvern Instruments, UK). The various glycerosomal dispersions were properly diluted with phosphate buffer solution, pH 7.4 to prevent multiple scattering effects. Samples were diluted and placed in disposable polystyrene cuvettes and measured at 173° fixed backscattering angle at 25°C. The mean vesicle diameter (Z-average) and PDI were measured for each batch and presented as mean ± SD. The results were repeated three times (n = 3) [26].

Zeta Potential:

Surface charge characterization of each glycerosomal dispersion was performed by electrophoretic light scattering on a Malvern Zetasizer Nano ZS (Malvern Instruments, UK) to gauge colloidal stability. Prior to measurement, each formulation was diluted to an appropriate scattering intensity and loaded into a disposable folded capillary zeta cell (DTS1070), ensuring no air entrapment within the detection chamber. All readings were acquired under thermostatic control at 25°C, and the electrokinetic data obtained were used to assess the magnitude of inter-vesicular electrostatic repulsion across all glycerosomal batches. Each formulation was independently analyzed on three separate occasions (n = 3), with values expressed as mean ± SD [27].

Entrapment Efficiency (EE%):

The fraction of entrapment was measured by ultracentrifugation after the separation of free and vesicle-entrapped fraction of drug in the fabricated glycerosomal formulations. The glycerosomal dispersions were centrifuged at 15,000 rpm for 45 minutes at 4°C with a refrigerated ultracentrifuge (Beckman Coulter, Model Optima XE-90, USA). Supernatant free drug was carefully separated and

Journal of Molecular Science
Journal of Molecular Science
Volume 36 Issue 2, Year of Publication 2026, Page 431-445
DoI-10.004687/1000-9035.2026.053

spectrophotometerically quantified at the predetermined λmax by referring to the pre-validated calibration curve. The entrapment efficiency was determined by the following equation:

$$\text{Entrapment Efficiency (\%)} = \left[\frac{(\text{Total drug added-Free drug in supernatant})}{\text{Total drug added}}\right]$$

All measurements were performed in triplicate (n = 3) and expressed as mean ± SD [28].

Drug Loading Capacity (DLC%):

The Glycerosomal formulations were drug loaded to determine drug content per unit weight of total lipid. The total encapsulated drug content in the pellet from the ultracentrifugation was released by dissolving in Methanol and the amount of drug released was quantified spectrophotometrically using the pre-validated calibration curve at the determined λ_{max}. The drug loading capacity was determined by the equation below:

$$\text{Drug Loading Capacity (\%)} = \left(\frac{\text{Weight of drug in vesicle}}{\text{Total weight of lipid used}}\right)\times 100$$

All determinations were carried out in triplicate (n = 3) and expressed as mean ± SD [29].

Morphological Characterization by Scanning Electron Microscopy:

Nanoscale surface architecture and three-dimensional structural features of the optimized glycerosomal formulation were examined by scanning electron microscopy (SEM), performed on a JEOL JSM-6390LV instrument (JEOL, Japan). A suitably diluted aliquot of the glycerosomal dispersion was deposited as a single droplet onto a polished silicon wafer substrate and left to desiccate under ambient conditions. To eliminate surface charge accumulation and maximize secondary electron emission, the dried specimen was sputter-coated with a nanometric gold-palladium film within a high-vacuum deposition chamber. Micrographs were acquired at an accelerating beam voltage of 15 to 20 kV across multiple magnification levels, enabling comprehensive visual evaluation of vesicle geometry, external surface texture, and the physical integrity of the glycerosomal architecture [30].

Surface pH Determination:

The surface pH of the Tazarotene loaded glycerosomal formulations was determined to evaluate the skin compatibility of their formulations because those formulations with a pH significantly lower or higher than the physiological skin pH (4.5-6.5) might be irritating after topical application. A calibrated digital pH electrode (Eutech Instruments, Model pH 510, Singapore) was immediately inserted into each glycerosomal dispersion to measure the pH at room temperature after calibration with pH 4.0 and pH 7.0 standard buffer solutions. The pH of each batch of the formulation was measured three times (n = 3) and reported as mean ± SD [31].

Drug Content Determination:

To verify batch-level fidelity of tazarotene incorporation within the glycerosomal vesicular matrix, drug content was quantified across all formulations using UV-Vis absorption spectrophotometry. An accurately weighed portion of each batch was introduced into a 10 mL graduated volumetric flask, into which methanol was added as a bilayer-disrupting solvent to lyse vesicular membranes; subsequent ultrasonic bath treatment for 10 minutes ensured complete extraction of the sequestered drug into solution. The resulting dispersion was gravity-filtered through Whatman grade 41 filter paper to remove insoluble residues, and the recovered filtrate was stepwise diluted with phosphate buffer (pH 7.4) to bring the drug concentration within the instrument's quantifiable detection window. Spectral absorbance at the confirmed λmax was recorded and tazarotene levels were back-calculated against a pre-validated concentration-response curve. Drug content was normalized to the nominal theoretical load and expressed as a percentage thereof. Independent replicate analyses were performed on three separate occasions per batch (n = 3), with findings presented as mean ± SD [32].

In Vitro Drug Release Study:

Tazarotene permeation kinetics from all glycerosomal batches were assessed using a static vertical Franz diffusion cell configured with a nominal permeation area of 2.0 cm^2 and an acceptor compartment capacity of 15 mL. A cellulose acetate barrier (MWCO 12,000–14,000 Da) was pre-hydrated by soaking in phosphate buffer (pH 7.4) for no less than 12 hours to ensure dimensional stability before mounting. Since tazarotene is a highly lipophilic retinoid, the acceptor compartment was charged with a hydroalcoholic medium (phosphate buffer pH 7.4/ethanol, 80:20 v/v) to maintain adequate dissolution capacity throughout the run. All cells were held at 37 ± 0.5°C in a temperature-regulated environment with the acceptor fluid under constant agitation at 600 rpm. One milligram of tazarotene formulated as a glycerosomal dispersion was deposited into the donor chamber, with the barrier maintained flush against the acceptor surface. At nine pre-defined sampling points spanning 0.5 to 12 hours, 1 mL of acceptor fluid was removed and replenished with an identical volume of freshly thermoequilibrated medium to uphold non-saturation conditions. Each sample was passed through Whatman 41 filter paper and analyzed spectrophotometrically at the confirmed λmax against a pre-established absorbance curve. Accumulated release at every interval was expressed

Journal of Molecular Science
Volume 36 Issue 2, Year of Publication 2026, Page 431-445
DoI-10.004687/1000-9035.2026.053

as a cumulative fraction of the loaded dose and plotted against elapsed time. Three fully independent experimental runs (n = 3) were completed, and outcomes are presented as mean ± SD [33].

Characterization of Glycerosomal gel:

Physical Appearance and Organoleptic Evaluation:

Organoleptic and physical evaluation of the prepared Tazarotene glycerosomal gel batches (GG1-GG4) was done by visual and sensory analysis. All batches were checked for colour against a white background and under daylight lighting conditions, clarity and homogeneity (by visual examination for the presence of lumps, aggregates or phase separating) and texture (by gently rubbing a small amount between the thumb and forefinger to check for smoothness and consistency of the batch). Odor was subjected to careful olfactory examination at a safe distance. During the texture evaluation grittiness or undispersed particles were also observed [34].

pH Determination:

Each Tazarotene glycerosomal gel batch (GG1 to GG4) was measured for its pH with a calibrated digital pH meter (Eutech Instruments Model pH 510, Singapore) using the pH standard solutions of pH 4 and pH 7 as buffer prior to measurement. About 0.5 g of gel formulations were made into dispersions in 50 ml of freshly prepared carbon dioxide-free distilled water and the electrode was dipped directly into the gel dispersion at room temperature. After a steady pH reading was achieved, the pH was noted. All experiments were repeated 3 times (n = 3) and data are given as mean ± SD [34].

Drug Content Determination:

Batch-wise tazarotene assay across the four glycerosomal gel formulations (GG1–GG4) was undertaken to establish the degree of uniform drug loading achieved during preparation. From each batch, a mass-calibrated gel portion equivalent to a nominal tazarotene content of 1 mg was introduced into a graduated flask pre-charged with methanol as the extracting solvent. The vessel was then immersed in a sonication bath for 10 minutes to achieve bilayer lysis and quantitative liberation of encapsulated drug into the methanolic phase. Particulate debris was eliminated by filtration through Whatman grade 41 paper, and the clarified eluate was serially diluted with phosphate buffer (pH 7.4) to attain a concentration amenable to optical detection. Absorbance at the drug's confirmed λmax was captured on a UV-Vis spectrophotometer, and tazarotene content was derived from a pre-validated linear response function. All outcomes were normalized to the nominal drug load and expressed as percentage recovery of the theoretical content. Three independent assay runs were completed per batch (n = 3), with results presented as mean ± SD [35].

Viscosity and Rheological Studies:

The viscosity and rheological behavior of Tazarotene glyc. gel batches (GG1-GG4) were measured with Brookfield viscometer with the spindle No. S64. For each sample of gel, it was transferred to the viscometer cup and allowed to equilibrate for 5 min at 25 ± 0.5°C before the measurement. The measurement was made at a predetermined spindle speed (50 rpm) and the reading was subsequently stabilised showing a viscosity reading in centipoise (cP). Rheological behaviour was also investigated by plotting a rheogram of shear stress versus shear rate and a comparison of the obtained curve with the other typical pseudoplastic curve of Carbopol-based gel systems was carried out. All measurements were done in triplicate (n = 3) and are presented as mean ± SD [36].

Spreadability:

The spreadability characteristics of each batch of the Tazarotene glycerosomal gel (GG1–GG4) was assessed in a spreadability test machine comprising two glass slides and a standard weight. 0.5g of each gel was dispensed in a 1cm glass diameter circle in one slide, covered with a second known weight glass and compressed for 5 minutes using a 500g weight so as to create uniform thickness. The weights of 20 g, 40 g and 60 g were then added one at a time and the time taken for the upper glass of the set to fall (by a fixed distance of 7.5 cm) was measured using a stopwatch. Spreadability (S) was determined by the following equation:

$$S = M \times \frac{L}{T}$$

The spreadability S (g·cm/s) is a calculated value using the applied weight M (g), the distance travelled L (cm) and the time taken T (s). All tests were repeated three times (n = 3) and the values were reported as Mean ± SD [37].

In Vitro Drug Release Study of Glycerosomal Gel:

Tazarotene release from each of the four glycerosomal gel batches (GG1–GG4) was characterized using a static Franz diffusion cell (active permeation area 2.0 cm^2; acceptor phase capacity 15 mL). Each gel, loaded with a nominal tazarotene dose of 1 mg, was packed into the donor chamber and partitioned from the acceptor compartment by a regenerated cellulose acetate barrier (MWCO 12,000–14,000 Da) pre-soaked for 12 hours in phosphate buffer (pH 7.4). Owing to the

Journal of Molecular Science
Volume 36 Issue 2, Year of Publication 2026, Page 431-445
DoI-10.004687/1000-9035.2026.053

pronounced lipophilicity of tazarotene, a hydroalcoholic acceptor medium was employed phosphate buffer (pH 7.4)/ethanol (80:20 v/v) to ensure non-saturating dissolution conditions across the full study window. The assembled cell was operated at 37 ± 0.5°C with the acceptor fluid under continuous rotational mixing at 600 rpm. At nine pre-defined collection points spanning 0.5 to 12 hours, a 1 mL portion was drawn from the acceptor compartment and promptly substituted with a matching volume of thermostatted fresh medium to uphold non-saturating conditions until the terminal collection. Every retrieved fraction was spectrophotometrically quantified at the drug's verified λmax, and the cumulative fraction released at each time point was calculated and rendered as a drug release time-course. A plain tazarotene gel devoid of any vesicular carrier served as a simultaneous comparator to quantify the release advantage conferred by glycerosomal architecture. Each complete experimental set was independently replicated three times (n = 3), with findings conveyed as mean ± SD [38].

Stability Studies:

Long-term physical and chemical robustness of the optimized tazarotene glycerosomal gel was interrogated through an accelerated stress protocol conducted in accordance with ICH Q1A(R2) guidelines over a 90-day observation window. The formulation was dispensed into amber-tinted glass containers to minimize photodegradation and housed within a climate-controlled stability unit (Thermolab Scientific Equipments, India) regulated at 40 ± 2°C and 75 ± 5% relative humidity. Aliquots were retrieved at monthly checkpoints spanning the zero to three-month period and subjected to comprehensive quality profiling encompassing macroscopic appearance, pH, drug assay, rheological behavior, spreadability, vesicular diameter, and encapsulation efficiency each conducted according to the respective analytical procedures documented earlier in this work. Every quality attribute was independently assessed across three replicate preparations (n = 3), with outcomes tabulated as mean ± SD to detect any statistically meaningful drift in formulation performance over the storage duration [39].

Statistical Analysis:

The values of all experimental data collected while formulating, optimizing and evaluating Tazarotene loaded glycerosomes and Tazarotene-Glycerosomal Gel are reported as mean ± standard deviation (SD) (n = 3). Design-Expert® software (Version 13, Stat-Ease Inc., Minneapolis, USA) was used for statistical analysis of data that included ANOVA and response surface methodology. GraphPad Prism (Version 9.0) was used for the comparative analysis between groups with $p<0.05$ being statistically significant [40].

RESULTS AND DISCUSSION:

RESULTS:

Calibration Curve Determination:

The calibration curve of Tazarotene in phosphate buffer at pH 7.4 shows that the regression coefficient (R^2 = 0.9993), obtained within the range of 5–30 µg/ml, proved to be excellent, indicating good linear correlation between concentration and absorbance, with a good linear relationship. The slope and intercept values led to validation of this method for its sensitivity and minimal systematic error, thus proving this method to be suitable for quantitative estimation of the next analytical studies.

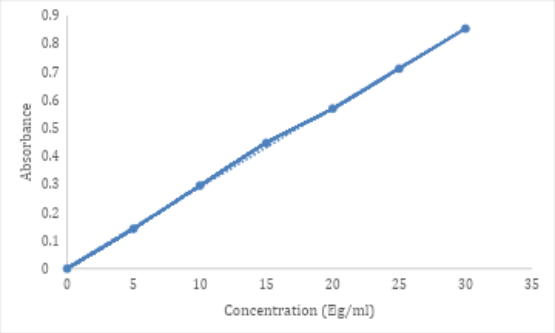

Figure 1: Calibration Curve of Tazarotene in Phosphate Buffer pH 7.4

Solubility Study:

The solubility study showed Tazarotene was practically insoluble in distilled water (0.002 ± 0.0003 mg/ml) and phosphate buffers, and freely soluble in methanol (285.6 ± 12.4 mg/ml), ethanol (156.8 ± 9.7 mg/ml) and acetone (312.4 ± 15.2 mg/ml) indicating its highly lipophilic nature; as indicated in Table 4. Glycerosomes formulation was possible owing to its slight solubility in glycerol (2.8 ± 0.4 mg/ml).

Table 4: Solubility Study of Tazarotene in Various Solvents

Sr. No.	Solvent	Solubility (mg/ml)	Inference
1	Distilled water	0.002 ± 0.0003	Practically insoluble
2	Phosphate buffer pH 7.4	0.010 ± 0.0015	Practically insoluble
3	Phosphate buffer pH 5.5	0.015 ± 0.0021	Very slightly soluble
4	Methanol	285.6 ± 12.4	Freely soluble
5	Ethanol	156.8 ± 9.7	Freely soluble
6	Acetone	312.4 ± 15.2	Freely soluble
7	Chloroform	68.5 ± 5.8	Soluble
8	Glycerol	2.8 ± 0.4	Slightly soluble

All values are expressed as mean ± SD

DSC Analysis:

The DSC thermogram of pure Tazarotene showed a sharp endothermic peak at 97.65°C, indicating that Tazarotene is crystalline with high purity as shown

Journal of Molecular Science
Volume 36 Issue 2, Year of Publication 2026, Page 431-445
DoI-10.004687/1000-9035.2026.053

in Figure 2. The physical mixture showed peaks at 91.43°C and 203.42, which suggested small shifts likely due to excipients interaction, but the peaks observed in the physical mixture were similar to the peaks observed in the non-interacting peaks, confirming the compatibility between the drug and excipients and suitability for formulation development.

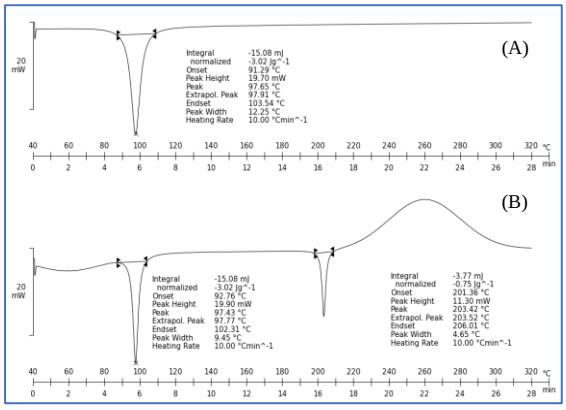

Figure 2: Representative DSC thermograms illustrating heat flow responses of (A) pure tazarotene exhibiting a single endothermic transition at 97.65°C, and (B) its physical admixture with excipients displaying dual thermal events at 91.43°C and 203.42°CFTIR Analysis

The FTIR spectra of pure Tazarotene showed characteristic absorption bands which recognized the major functional group of Tazarotene, with the integrity of its structure, as is shown in Fig 3. It was observed that in the physical mixture, there was no significant shift of peak positions, disappearance or appearance of any principal peak of the drug and the excipients selected for the formulation, which indicated absence of chemical incompatibility between Tazarotene and the selected excipients used for preparing glycerosome and hence their combined use was considered safe.

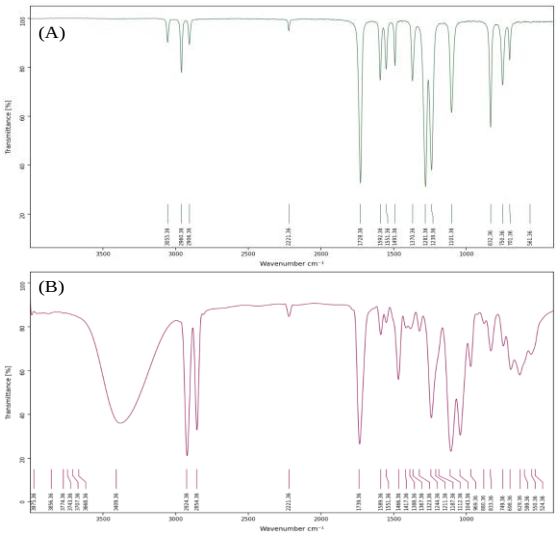

Figure 3: FTIR spectra of (A) Pure extract and (B) Physical mixture

Results of Characterization of Tazarotene loaded glycerosomes:

The size of vesicles obtained from all seventeen batches varied from 143.4 ± 1.2 nm for F11 to 187.9 ± 2.0 nm for F8 whereas PDI values ranged between 0.155–0.248 indicating the vesicles had an acceptable size uniformity as shown in Table 5. The z-average potential values were between −18.3 and −30.2 mV which are satisfactory for electrostatic stability. Entrapment efficiency ranged from 82.3 ± 0.7% (F7) to 92.7 ± 0.4% (F9), with the optimized batch F4 demonstrating vesicle size of 152.4 ± 1.5 nm, PDI of 0.176 ± 0.007, zeta potential of −24.7 ± 1.3 mV, and EE of 90.9 ± 0.4%.

Table 5: Vesicle Size, PDI, Zeta Potential and Entrapment Efficiency of F1–F17

Batch	Vesicle Size (nm)	PDI	Zeta Potential (mV)	EE (%)
F1	183.2 ± 1.8	0.168 ± 0.008	−28.4 ± 1.2	88.5 ± 0.6
F2	146.5 ± 1.4	0.234 ± 0.011	−19.6 ± 0.9	84.9 ± 0.5
F3	152.8 ± 1.6	0.248 ± 0.009	−18.3 ± 1.1	83.1 ± 0.7
F4	152.4 ± 1.5	0.176 ± 0.007	−24.7 ± 1.3	90.9 ± 0.4
F5	155.8 ± 1.3	0.192 ± 0.006	−23.1 ± 0.8	89.4 ± 0.5
F6	174.3 ± 2.1	0.204 ± 0.008	−22.4 ± 1.0	83.1 ± 0.6
F7	151.6 ± 1.4	0.228 ± 0.010	−20.3 ± 0.9	82.3 ± 0.7
F8	187.9 ± 2.0	0.158 ± 0.007	−30.2 ± 1.4	87.3 ± 0.5
F9	170.4 ± 1.9	0.162 ± 0.008	−27.8 ± 1.1	92.7 ± 0.4
F10	156.3 ± 1.2	0.194 ± 0.005	−23.4 ± 0.7	89.6 ± 0.5
F11	143.4 ± 1.2	0.218 ± 0.009	−21.5 ± 1.0	85.1 ± 0.6
F12	155.7 ± 1.4	0.191 ± 0.006	−23.2 ± 0.8	89.5 ± 0.4
F13	173.1 ± 1.7	0.155 ± 0.007	−29.1 ± 1.2	92.5 ± 0.5
F14	162.5 ± 1.8	0.198 ± 0.008	−22.8 ± 0.9	87.1 ± 0.6
F15	156.1 ± 1.3	0.193 ± 0.006	−23.3 ± 0.7	89.3 ± 0.4
F16	163.8 ± 1.6	0.187 ± 0.007	−24.1 ± 1.1	86.1 ± 0.5
F17	156.2 ± 1.5	0.192 ± 0.005	−23.1 ± 0.8	89.5 ± 0.5

All values are expressed as mean ± SD, n=3

The drug loading capacity of all seventeen batches varied from 1.98 ± 0.07 % (F8) to 3.87 ± 0.11 % (F11) with an inverse relationship seen between the concentration of phosphatidylcholine and DLC, as outlined in Table 6. The surface pH of all batches was found to be between 6.73 ± 0.02 and 6.94 ± 0.03 which is in the physiologically acceptable pH range of the skin (4.5-7.0). Drug content remained consistently high across all batches, ranging from 96.4 ± 0.7% to 99.3 ± 0.5%, with the optimized

Journal of Molecular Science
Volume 36 Issue 2, Year of Publication 2026, Page 431-445
DoI-10.004687/1000-9035.2026.053

batch F4 exhibiting DLC of 2.75 ± 0.09%, surface pH of 6.85 ± 0.02, and drug content of 99.1 ± 0.4%.

Table 6: Drug Loading Capacity, Surface pH and Drug Content of F1–F17

Batch	DLC (%)	Surface pH	Drug Content (%)
F1	2.01 ± 0.08	6.92 ± 0.03	98.4 ± 0.6
F2	3.86 ± 0.11	6.78 ± 0.02	97.2 ± 0.5
F3	3.78 ± 0.10	6.81 ± 0.03	96.8 ± 0.7
F4	2.75 ± 0.09	6.85 ± 0.02	99.1 ± 0.4
F5	2.71 ± 0.07	6.88 ± 0.02	98.6 ± 0.5
F6	2.52 ± 0.08	6.76 ± 0.03	97.5 ± 0.6
F7	3.74 ± 0.10	6.73 ± 0.02	96.4 ± 0.7
F8	1.98 ± 0.07	6.94 ± 0.03	99.3 ± 0.5
F9	2.11 ± 0.08	6.89 ± 0.02	98.9 ± 0.4
F10	2.72 ± 0.07	6.87 ± 0.02	98.7 ± 0.5
F11	3.87 ± 0.11	6.82 ± 0.03	97.8 ± 0.6
F12	2.71 ± 0.07	6.86 ± 0.02	98.5 ± 0.4
F13	2.10 ± 0.08	6.91 ± 0.02	99.2 ± 0.5
F14	2.64 ± 0.09	6.84 ± 0.03	98.1 ± 0.6
F15	2.71 ± 0.07	6.88 ± 0.02	98.6 ± 0.4
F16	2.61 ± 0.08	6.79 ± 0.03	97.9 ± 0.5
F17	2.71 ± 0.07	6.87 ± 0.02	98.4 ± 0.5

All values are expressed as mean ± SD, n=3

Optimization of tazarotene loaded glycerosomes

Vesicle Size (Y_1)

The quadratic model was selected as the most appropriate model for vesicle size, as presented in Table 7. The sequential p-value of < 0.0001, adjusted R^2 of 0.9996 and predicted R^2 of 0.9986 indicated high model predictability. The overall model F-value of 193.99 ($p < 0.0001$) indicated high significance (Table 8) and the non-significant lack of fit ($F = 0.9826$, $p = 0.4850$) confirmed model fitting. Phosphatidylcholine (X_1) exerted the most dominant influence on vesicle size ($F = 27203.18$, $p < 0.0001$), followed by glycerol (X_2; $F = 3942.93$, $p < 0.0001$) and Tween 80 (X_3; $F = 3022.58$, $p < 0.0001$). The interaction X_1X_2 was significant ($F = 578.05$, $p < 0.0001$), whereas the other interactions (X_1X_3, X_2X_3) were not significant. All quadratic terms were highly significant ($p < 0.0001$), and this indicated highly pronounced non-linear curvature of the response. $Y_1 = +156.02 + 15.04A - 5.72B - 5.01C - 3.10AB - 0.1750AC + 0.1000BC + 3.98A^2 + 4.10B^2 + 3.13C^2$ The positive coefficient of X_1 (+15.04) was the highest, which suggested that when phosphatidylcholine was increased in turn, the number of bilayers forming multilamellar vesicles increased, resulting in their growth. The negative values of coefficients X_2 (−5.72) and X_3 (−5.01) indicated the size reduction effect by membrane-fluidizing effect and surfactant action, respectively. The negative interaction coefficient X_1X_2 (−3.10) is a significant value that implies that increasing phosphatidylcholine concentration led to increased size reduction. All the quadratic terms were positive suggesting that the relationships were parabolas with a peak in vesicle size at intermediate values. The interaction between X_1 and X_2 exhibits elliptical patterns as illustrated by the contour plots presented (Figure 4A1–A3) and the three-dimensional response surface plots presented (Figure 5A1–B3), respectively, show the curve along the X_1 axis and the valley along the intermediate concentrations of glycerol.

Encapsulation Efficiency (Y_2):

Quadratic model was the best model for describing the encapsulation efficiency, as seen in Table 7, with the p-value < 0.0001, adjusted R^2 of 0.9970, and predicted R^2 of 0.9839, respectively. The model F value of 599.51, with the associated significance of $p < 0.0001$, confirmed that the model was significant overall (Table 8) and that lack of fit was not significant ($F = 4.10$, $p = 0.1031$) indicating adequate model fitting. Phosphatidylcholine remained the most influential factor ($F = 2704.91$, $p < 0.0001$), followed by glycerol ($F = 1164.91$, $p < 0.0001$) and Tween 80 ($F = 676.23$, $p < 0.0001$). Interaction terms X_1X_2 ($F = 64.72$, $p < 0.0001$) and X_1X_3 ($F = 33.02$, $p = 0.0007$) were significant, while X_2X_3 was non-significant ($p = 0.0551$). All quadratic terms were highly significant ($p<0.0001$), further indicating that the behavior in all variables was non-linear. $Y_2 = +89.46 + 3.20A + 2.10B + 1.60C + 0.7000AB + 0.5000AC + 0.2000BC - 1.08A^2 - 1.58B^2 - 1.08C^2$ A positive linear coefficient for X_1 (+3.20), X_2 (+2.10) and X_3 (+1.60) suggested that each of the three components contributed positively to increase the EE for tazarotene, whereby the phosphatidylcholine played a dominant role by increases the hydrophobic bilayer domain for the entrapment of tazarotene. The results of the negative quadratic coefficients ($A^2 = -1.08$, $B^2 = -1.58$ and $C^2 = -1.08$) indicated that the efficiency of encapsulation was maximum in intermediate ranges and decreased at high concentrations. Elliptical patterns were observed for significant interaction X_1X_2 and X_1X_3, and a large plateau was found for the insignificant interaction X_2X_3 with contour plots (Figure 4B1–B3), and three-dimensional response surface plots (Figure 5B1–B3) showed a typical dome shape with maximum encapsulation at higher phosphatidylcholine and intermediate glycerol concentrations.

Table 7: Model Fit Summary for Optimization of Tazarotene-Loaded Glycerosomes

Response	Model	Sequential p-value	Lack of Fit p-value	Adjusted R^2	Predicted R^2
Vesicle Size (Y_1)	Quadratic	< 0.0001	0.4850	0.9996	0.9986
Encapsulation Efficiency (Y_2)	Quadratic	< 0.0001	0.1031	0.9970	0.9839

Table 8: ANOVA Summary for Quadratic Models of Tazarotene-Loaded Glycerosomes

Source	Sum of Squares	df	Mean Square	F-value	p-value	Significance

Journal of Molecular Science
Volume 36 Issue 2, Year of Publication 2026, Page 431-445
DoI-10.004687/1000-9035.2026.053

Vesicle Size (Y_1)						
Model	2510.10	9	278.90	193.99	< 0.0001	Significant
A-Phosphatidylcholine	1809.01	1	1809.01	27203.18	< 0.0001	Significant
B-Glycerol	262.20	1	262.20	3942.93	< 0.0001	Significant
C-Tween 80	201.00	1	201.00	3022.58	< 0.0001	Significant
AB	38.44	1	38.44	578.05	< 0.0001	Significant
AC	0.1225	1	0.1225	1.84	0.2168	Not Significant
BC	0.0400	1	0.0400	0.6015	0.4634	Not Significant
A^2	66.61	1	66.61	1001.69	< 0.0001	Significant
B^2	70.87	1	70.87	1065.64	< 0.0001	Significant
C^2	41.18	1	41.18	619.31	< 0.0001	Significant
Residual	0.4655	7	0.0665			
Lack of Fit	0.1975	3	0.0658	0.9826	0.4850	Not Significant
Pure Error	0.2680	4	0.0670			
Cor Total	2510.57	16				
Encapsulation Efficiency (Y_2)						
Model	163.41	9	18.16	599.51	< 0.0001	Significant
A-Phosphatidylcholine	81.92	1	81.92	2704.91	< 0.0001	Significant
B-Glycerol	35.28	1	35.28	1164.91	< 0.0001	Significant
C-Tween 80	20.48	1	20.48	676.23	< 0.0001	Significant
AB	1.96	1	1.96	64.72	< 0.0001	Significant
AC	1.0000	1	1.0000	33.02	0.0007	Significant
BC	0.1600	1	0.1600	5.28	0.0551	Not Significant
A^2	4.91	1	4.91	162.16	< 0.0001	Significant
B^2	10.51	1	10.51	347.07	< 0.0001	Significant
C^2	4.91	1	4.91	162.16	< 0.0001	Significant
Residual	0.2120	7	0.0303			
Lack of Fit	0.1600	3	0.0533	4.10	0.1031	Not Significant
Pure Error	0.0520	4	0.0130			
Cor Total	163.62	16				

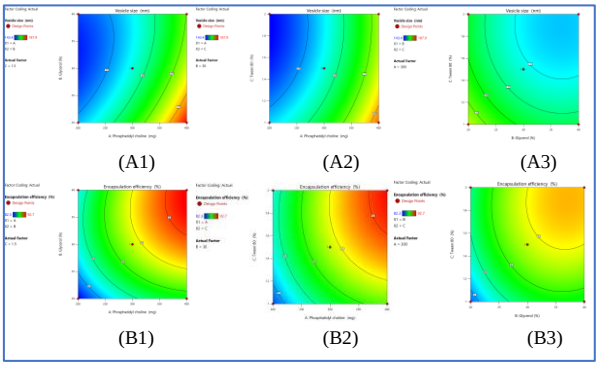

Figure 4: Contour plots showing the effect of independent variables on (A1–A3) vesicle size (nm) and (B1–B3) encapsulation efficiency (%) of Tazarotene-loaded glycerosomes. (A1/B1) Combined effect of phosphatidylcholine concentration (mg) and glycerol concentration (%) at fixed Tween 80 concentration (1.5% v/v); (A2/B2) combined effect of phosphatidylcholine concentration (mg) and Tween 80 concentration (%) at fixed glycerol concentration (30% v/v); (A3/B3) combined effect of glycerol concentration (%) and Tween 80 concentration (%) at fixed phosphatidylcholine concentration (300 mg).

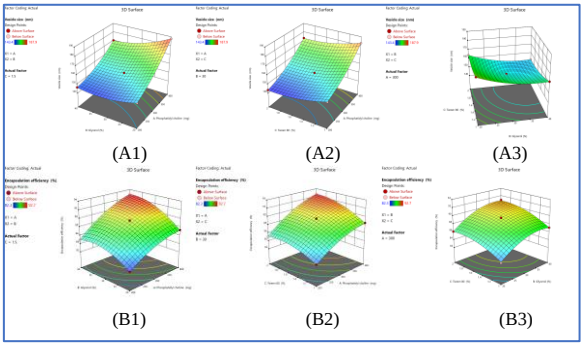

Figure 5: Three-dimensional response surface plots showing the effect of independent variables on (A1–A3) vesicle size (nm) and (B1–B3) encapsulation efficiency (%) of Tazarotene-loaded glycerosomes. (A1/B1) Combined effect of phosphatidylcholine concentration (mg) and glycerol concentration (%) at fixed Tween 80 concentration (1.5% v/v); (A2/B2) combined effect of phosphatidylcholine concentration (mg) and Tween 80 concentration (%) at fixed glycerol concentration (30% v/v); (A3/B3) combined effect of glycerol concentration (%) and Tween 80 concentration (%) at fixed phosphatidylcholine concentration (300 mg).

Journal of Molecular Science
Volume 36 Issue 2, Year of Publication 2026, Page 431-445
DoI-10.004687/1000-9035.2026.053

Validation of Statistical Model:

The strong correlation between predicted and experimental values for both responses supported the high predictive power of the quadratic models developed (see Table 9). The relative errors of vesicle size and EE were 1.19% and 0.66%, respectively, which are within the acceptable limit of 5%. A desirability value of 1 indicated that the optimized batch F4 met both optimization goals at once, which is minimized vesicle size and maximized encapsulations efficiency.

Table 9: Validation of Optimized Formulation Batch Predicted vs. Experimental Values with Percentage Relative Error and Desirability

Batch	Response	Predicted value	Experimental value	% Relative error	Desirability
F4	Vesicle size	154.242	152.4	1.19	1
	Entrapment efficiency	91.500	90.9	0.66	

SEM Analysis:

It was concluded that the optimized batch F4 had uniform and well defined spherical vesicles without any aggregation or fusion and which also appeared at an even distribution (Figure 6). The vesicles demonstrated a characteristic core-shell structure and surface morphology showing smooth and intact surfaces, typical features of glycerosomes. The particle size obtained in the experiment was found to be close to the data obtained from dynamic light scattering, which indicates that the vesicles, formed in the experiment were of nanometric size and remained intact in solutions.

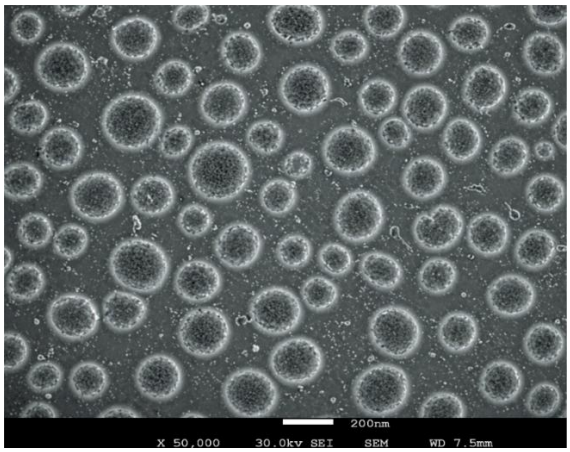

Figure 6: SEM of optimized batch (F4)

Results of in vitro drug release:

The results of in vitro drug release are shown.The in vitro drug release results are presented. Figure 7 shows that all the 17 batches of glycerosome gave sustained drug release profile in absence of initial burst effect throughout the study period which confirmed the intact vesicular encapsulation during the study. The optimized batch F4 gave 75.8 ± 0.5% cumulative drug release at 12 hours, with an even gradual release, proving the formulation to be suitable for a sustained topical release of Tazarotene.

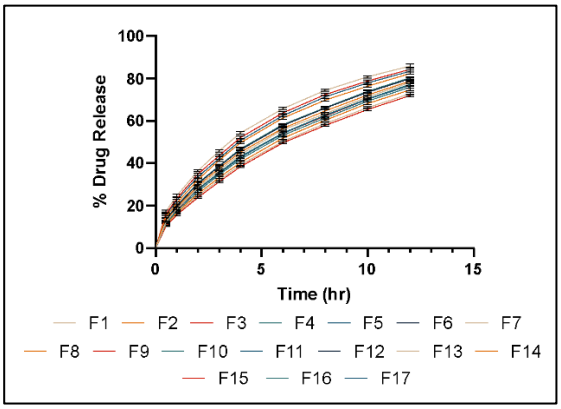

Figure 7: In vitro drug release profile of all glycerosomes batches

Results of Characterization of Glycerosomal gel

Results of Physical Appearance:

Table 10 shows that all four batches of glycerosomal gels (GG1– GG4) were consistent and free from lumps, grittiness, phase separation and syneresis indicating satisfactory physical quality, in the form of clear, smooth, pale yellow, homogeneous gels. As the amount of Carbopol 934 increased from GG1 to GG4, the consistency increased progressively and the best consistency was observed with GG3.An increase in consistency occurred from GG1 to GG4 as the concentration of Carbopol 934 increased, and the most desirable consistency was found in GG3 of all the prepared batches.

Table 10: Physical Appearance and Organoleptic Evaluation of Tazarotene Glycerosomal Gel Batches GG1–GG4

Parameter	GG1	GG2	GG3	GG4
Color	Pale yellow	Pale yellow	Pale yellow	Pale yellow
Clarity	Clear	Clear	Clear	Clear
Homogeneity	Homogeneous	Homogeneous	Homogeneous	Homogeneous
Texture	Smooth, soft	Smooth, soft	Smooth, uniform	Smooth, firm
Consistency	Low viscous, easily spreadable	Moderately viscous, spreadable	Viscous, smooth	Highly viscous, stiff
Odor	Odorless	Odorless	Odorless	Odorless
Grittiness	Absent	Absent	Absent	Absent
Phase Separation	Absent	Absent	Absent	Absent
Syneresis	Absent	Absent	Absent	Absent

Results of Physicochemical characterization:

Journal of Molecular Science
Volume 36 Issue 2, Year of Publication 2026, Page 431-445
DoI-10.004687/1000-9035.2026.053

All the batches of gels were found to be within the skin compatible range of pH between 6.12 ± 0.02 to 6.31 ± 0.03 as shown in Table 11. The content of all the batches was at a uniform high level ranging from 97.4% to 98.6%. As the viscosity of the doughs increased from 1248 ± 18.4 cP (GG1) to 7486 ± 38.4 cP (GG4), the spreadability decreased from 28.64 ± 0.42 to 11.32 ± 0.26 g·cm/s, with GG3 showing the best combination of both parameters.

Table 11: pH, Drug Content, Viscosity and Spreadability of Tazarotene Glycerosomal Gel Batches GG1–GG4

Parameter	GG1	GG2	GG3	GG4
pH	6.12 ± 0.02	6.18 ± 0.03	6.24 ± 0.02	6.31 ± 0.03
Drug Content (%)	97.4 ± 0.5	98.1 ± 0.4	98.6 ± 0.6	97.8 ± 0.5
Viscosity (cP)	1248 ± 18.4	2874 ± 22.6	4632 ± 31.2	7486 ± 38.4
Spreadability (g·cm/s)	28.64 ± 0.42	22.18 ± 0.38	16.74 ± 0.31	11.32 ± 0.26

All values are expressed as mean ± SD

Results of In vitro drug release of gel batches:

The cumulative release of the drugs from the glycerosomal gel batches showed a sustained release and ranged from 61.2 ± 0.5 % (GG4) to 76.4 ± 0.6 % (GG1) at 12 hrs. (refer Fig 8) Finally, GG3 showed a well-balanced release of 67.4 ± 0.6% at 12 hours without any burst effect, which indicates optimized sustained release and appropriate drug permeation, and was thus selected as the optimized gel formulation.

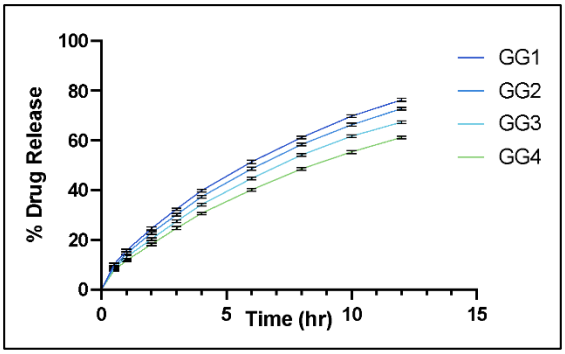

Figure 8: In vitro drug release profile of all batches of glycerosomal batches

Results of stability study:

Table 12 summarizes the results of all of the evaluated parameters of the optimized Tazarotene glycerosomal gel GG3 for three months of accelerated stability testing, during which the product showed physical and chemical stability. The pH of the formulation shifted slightly from 6.24 ± 0.02 to 6.17 ± 0.03 and the amount of the drug remained above 97% during the study. The size of the vesicles was marginally increased from 152.4 ± 1.5 to 157.1 ± 2.0 nm and entrapment efficiency decreased marginally from 90.9 ± 0.4% to 88.7 ± 0.5% which were statistically non-significant ($p > 0.05$) indicating acceptable formulation stability under ICH Q1A(R2) accelerated conditions.

Table 12: Stability Data of Optimized Tazarotene Glycerosomal Gel (GG3) at Accelerated Conditions

Parameter	0 Month	1 Month	2 Months	3 Months
Physical Appearance	Pale yellow, clear, homogeneous, smooth gel	Pale yellow, clear, homogeneous, smooth gel	Pale yellow, clear, homogeneous, smooth gel	Pale yellow, clear, homogeneous, smooth gel
Color Change	Absent	Absent	Absent	Absent
Phase Separation	Absent	Absent	Absent	Absent
pH	6.24 ± 0.02	6.21 ± 0.03	6.19 ± 0.02	6.17 ± 0.03
Drug Content (%)	98.6 ± 0.6	98.1 ± 0.5	97.6 ± 0.6	97.2 ± 0.5
Viscosity (cP)	4632 ± 31.2	4598 ± 28.4	4561 ± 30.6	4524 ± 29.8
Spreadability (g·cm/s)	16.74 ± 0.31	16.68 ± 0.28	16.52 ± 0.34	16.38 ± 0.30
Vesicle Size (nm)	152.4 ± 1.5	153.8 ± 1.6	155.2 ± 1.8	157.1 ± 2.0
Entrapment Efficiency (%)	90.9 ± 0.4	90.2 ± 0.5	89.4 ± 0.6	88.7 ± 0.5

All values expressed as mean ± SD, n=3

DISCUSSION:

The preformulation characterization of Tazarotene revealed that it is a white crystalline compound with a melting point of 97.4 ± 0.8°C, which matches the reported melting point. The UV spectrophotometric analysis confirmed that there was a well defined λ_{max} of 351 nm in phosphate buffer pH 7.4 with good linear regression ($R^2 = 0.9993$) ranging from 5 to 30 µg/ml, which was found to be suitable for further quantitative estimation, according to the guidelines given by the ICH Q2(R1) [41]. The physicochemical profile of Tazarotene and its reported log P value confirmed that the drug has a highly lipophilic nature, and solubility studies showed that the aqueous solubility of Tazarotene is nearly negligible (0.002 ± 0.0003mg/ml) while its solubility is high in organic solvents as stated in Table 4 below [41]. Its small solubility in glycerol (2.8 ± 0.4 mg/mL) supported its use as bilayer modifying agent instead of a solubilizing medium, a practice which was previously used in glycerosome studies under good scientific grounds [42]. To check crystallinity, DSC analysis was conducted on Tazarotene and physical mixture of Tazarotene, as shown in Figure 2, which exhibited an endothermic peak at 97.65°C without any loss of characteristic peaks of Tazarotene in DSC signals of physical mixture, suggesting thermodynamic incompatibility between the drug and excipients [43]. The results were also supported by FTIR spectral analysis that showed no change in

Journal of Molecular Science
Volume 36 Issue 2, Year of Publication 2026, Page 431-445
DoI-10.004687/1000-9035.2026.053

the main functional group peaks of both Tazarotene and the excipients in the physical mixture, as seen in Figure 3, indicating that there is no chemical incompatibility between the excipients and Tazarotene. The overall preformulation results provided a scientific basis for the rational design of the tazarotene loaded glycerosomes [44].

The Box-Behnken design was used to successfully optimize the vesicle size (Y_1) and encapsulation efficiency (Y_2) of the glycerosome formulation, where both the models generated were quadratic with high adjusted R^2 values of 0.9996 and 0.9970 respectively, and without lack of fit with P-values greater than 0.05 as can be seen in Table 7 and Table 8. Phosphatidylcholine concentration was the most significant factor affecting both responses, as has been reported for phospholipid-based vesicular systems where the lipid concentration is a factor determining the bilayer thickness and/or the drug entrapment capacity [45]. Glycerol and Tween 80 have been found to have a negative effect on vesicle size, consistent with previous studies with glycerosomes, which showed that glycerol incorporation into the lipid bilayer increased the fluidity of lipid membranes and decreased the size of vesicles, and the presence of Tween 80 led to homogenization by means of the surfactant. The optimized batch F4 obtained based on the calculation of desirability value 1 showed excellent model predictability with the percentage relative error lying within 1.19% and 0.66% (Table 9), and its parameters: Vesicle size: 152.4 ± 1.5 nm, PDI: 0.176 ± 0.007, Zeta potential: −24.7 ± 1.3 mV, EE: 90.9 ± 0.4%. (Table 5) [46]. The negative zeta potential values obtained for all batches support the concept that sufficient electrostatic repulsion, an important factor for long term colloidal stability, was achieved, consistent with previous studies on vesicular formulations, which established the minimum criteria for stability as being a zeta potential of either negative or positive values of 20 mV. The DLS results were confirmed by SEM imaging of the optimized batch F4 which showed the presence of discrete, spherical vesicles with smooth surface morphologies and core-shell architecture, as seen in Figure 6 [47]. In vitro studies of drug release from optimized glycerosomal dispersion found that release was sustained for 75.8 ± 0.5% of the drug after 12 hours with no burst effect due to the controlled diffusion of Tazarotene through the undisturbed multilamellar lipid bilayers, as shown in Figure 7. The formulations of the optimized glycerosomal dispersion prepared by incorporating the dispersion into Gel (GG1–GG4 containing 0.25%, 0.5%, 1.0% and 1.5% of Carbopol 934, respectively) were found to have satisfactory physical properties (Table 10, Table 11) as expected in topical gel formulations where GG3 (1.0% Carbopol 934) possesses optimal viscosity of 4632 ± 31.2 cP, spreadability of 16.74 ± 0.31 g·cm/s, a pH of 6.24 ± 0.02 and a drug content of 98.6 ± 0.6%, all of which corroborates with the previously reported optimum values for topical gel formulation [48]. In vitro drug release profile of GG3 at 12 h (Figure 8) was significantly lesser than the drug gel control confirming the sustained release effect provided by the glycerosomal encapsulation in the drug gel and found comparable to other vesicular drug gel systems reported in the recent literature. Based on the results of accelerated stability studies (Table 12), the developed Tazarotene glycerosomal gel exhibited excellent physical and chemical stability with only marginal, statistically insignificant changes in vesicle size (152.4 to 157.1 nm), EE (90.9–88.7%), pH, viscosity and spreadability indicating the developed Tazarotene glycerosomal gel is a robust and shelf-life appropriate well-tolerated topical platform for the management of acne [49].

CONCLUSION:

In the present study, the development and optimization of glycerosomes containing tazarotene were successfully carried out by Box-Behnken design and the concentrations of phosphatidylcholine, glycerol and Tween 80 were used as critical formulation parameters. The optimized batch F4 was loaded in a Carbopol 934-based gel (GG3), which had desirable physicochemical properties such as initial vesicle size (152.4 ± 1.5 nm), entrapment efficiency (90.9 ± 0.4%), sustained drug release over 12 hours and pH value suitable for skin application, suggesting its potential for improving the topical bioavailability of the drug and reducing the cutaneous irritation of the conventional Tazarotene preparations. Its ability to withstand accelerated conditions as per ICH Q1A(R2) further confirms its pharmaceutical robustness and shelf-life suitability. Another exciting clinical potential of the developed formulation is its potential to increase patient acceptance and treatment outcomes by decreasing the side effects of retinoids in the treatment of acne. Further work using ex vivo skin permeation, in vivo pharmacodynamic testing, and clinical safety testing is warranted to extend our understanding of the translational relevancy of this novel glycerosomal gel platform.

ABBREVIATIONS:

ANOVA: Analysis of Variance; BBD: Box-Behnken Design; DLC: Drug Loading Capacity; DLS: Dynamic Light Scattering; DSC: Differential Scanning Calorimetry; EE: Entrapment Efficiency; FTIR: Fourier Transform Infrared Spectroscopy; ICH: International Council for Harmonisation; MWCO: Molecular Weight Cut-Off; PDI: Polydispersity Index; RH: Relative Humidity; SEM:

Scanning Electron Microscopy; SD: Standard Deviation; TEA: Triethanolamine; UV: Ultraviolet Spectrophotometry; λmax: Wavelength of Maximum Absorption.

REFERENCES

1. Chen H, Zhang T c., Yin X l., Man J y., Yang X r., Lu M. Magnitude and temporal trend of acne vulgaris burden in 204 countries and territories from 1990 to 2019: an analysis from the Global Burden of Disease Study 2019. Br J Dermatol 2022; 186:673–83. https://doi.org/10.1111/bjd.20882.
2. Wang Y, Xiao S, Ren J, Zhang Y. Analysis of the epidemiological burden of acne vulgaris in China based on the data of global burden of disease 2019. Front Med 2022;9. https://doi.org/10.3389/fmed.2022.939584.
3. Zhu Z, Zhong X, Luo Z, Liu M, Zhang H, Zheng H, et al. Global, regional and national burdens of acne vulgaris in adolescents and young adults aged 10–24 years from 1990 to 2021: a trend analysis. Br J Dermatol 2025; 192:228–37. https://doi.org/10.1093/bjd/ljae352.
4. Guguluș DL, Vâță D, Popescu IA, Pătrașcu AI, Halip IA, Mocanu M, et al. The Epidemiology of Acne in the Current Era: Trends and Clinical Implications. Cosmetics 2025; 12:106. https://doi.org/10.3390/cosmetics12030106.
5. Vasam M, Korutla S, Bohara RA. Acne vulgaris: A review of the pathophysiology, treatment, and recent nanotechnology based advances. Biochem Biophys Rep 2023;36:101578. https://doi.org/10.1016/j.bbrep.2023.101578.
6. Wang C-H, Wang L-K, Tsai F-M. Exploring Potential Therapeutic Applications of Tazarotene: Gene Regulation Mechanisms and Effects on Melanoma Cell Growth. Curr Issues Mol Biol 2025;47:237. https://doi.org/10.3390/cimb47040237.
7. Shergill M, Ali MU, Abu-Hilal M. Comparison of the Efficacy of Clascoterone, Trifarotene, and Tazarotene for the Treatment of Acne: A Systematic Literature Review and Meta-Analysis. Dermatol Ther 2024;14:1093–102. https://doi.org/10.1007/s13555-024-01175-3.
8. Hegazy D, Fayed NM, Nour El-Din HT, Habib BA, Abdelrehim RT. Optimized Tazarotene Transfersomes Versus Previously Optimized Tazarotene Cubosomes: Exploring Their In Vivo Anti-Acne Activity in a Cutibacterium acnes Inflammatory Murine Model. BioNanoScience 2025;15:410. https://doi.org/10.1007/s12668-025-02009-y.
9. Kshirsagar SM, Shrestha N, Kipping T, Banga AK. Formulation development of tazarotene-loaded PLGA nanoparticles for follicular delivery in the treatment of inflammatory skin diseases. Eur J Pharm Biopharm 2024; 200:114346. https://doi.org/10.1016/j.ejpb.2024.114346.
10. Mohney LA, Singh R, Feldman SR. Tazarotene 0.045% Lotion: A Novel Retinoid Formulation. Ann Pharmacother 2022;56:1174–80. https://doi.org/10.1177/10600280211072155.
11. Choudhary V, Khan A, Shekhedwal S, Chauhan B, Singh R. Glycerosomes as advanced vesicular drug delivery systems for topical antifungal therapy: Formulation strategies and therapeutic potential. Drug Discov Dev 2026:1–16. https://doi.org/10.5530/ddd.2.2.7.
12. Aroffu M, Matricardi P, Meo CD, Valenti D, Ferraro M, Pace E, et al. Hyaluronan-cholesterol core–shell glycerosomes: innovative nanocarriers for mitigating smoke-induced oxidative stress and inflammation in the lungs. Int J Pharm 2026;695:126776. https://doi.org/10.1016/j.ijpharm.2026.126776.
13. Zhang Y, Liang R, Liu C, Yang C. Improved stability and skin penetration through glycethosomes loaded with glycyrrhetinic acid. Int J Cosmet Sci 2022; 44:249–61. https://doi.org/10.1111/ics.12771.
14. García FJG, Andreo AR, Manconi M, Manca ML, Matricardi P, di Meo C, et al. In vitro and in vivo efficacy evaluation of new self-assembling curcumin loaded nanohyaluronan-glycerosomes on wound restoring in health and diabetic rats. Int J Biol Macromol 2025; 315:144699. https://doi.org/10.1016/j.ijbiomac.2025.144699.
15. Singh R, Zeeshan F, Srivastava D, Awasthi H. A Discursive Review of Recent Development and Patents on Glycerosomes. Recent Pat Nanotechnol 2023; 17:183–9. https://doi.org/10.2174/1872210516666220328124450.
16. Salem HF, Kharshoum RM, Sayed OM, Abdel Hakim LF. Formulation design and optimization of novel soft glycerosomes for enhanced topical delivery of celecoxib and cupferron by Box–Behnken statistical design. Drug Dev Ind Pharm 2018; 44:1871–84. https://doi.org/10.1080/03639045.2018.1504963.
17. Anwer MdK, Alshdefat R, Akhtar J, Aleemuddin M. Punica granatum Loaded Glycerosomes for Antibacterial Effect in Skin Infections: Preparation, Optimization, In Vitro and In Vivo Characterization. BioNanoScience 2025; 15:294. https://doi.org/10.1007/s12668-025-01910-w.
18. Rahimpour E, Moradi M, Sheikhi-Sovari A, Rezaei H, Rezaei H, Jouyban-Gharamaleki V, et al. Comparative Drug Solubility Studies Using Shake-Flask Versus a Laser-Based Robotic Method. AAPS PharmSciTech 2023; 24:207. https://doi.org/10.1208/s12249-023-02667-9.
19. Zhu C, Zhang Y, Wu T, He Z, Guo T, Feng N. Optimizing glycerosome formulations via an orthogonal experimental design to enhance transdermal triptolide delivery. Acta Pharm 2022;72:135–46. https://doi.org/10.2478/acph-2022-0006.
20. Younes NF, Habib BA. Augmented local skin accumulation efficiency of sertaconazole nitrate via glycerosomal hydrogel: Formulation, statistical optimization, ex vivo performance and in vivo penetration. J Drug Deliv Sci Technol 2022; 72:103364. https://doi.org/10.1016/j.jddst.2022.103364.
21. Zaki RM, Alfadhel MM, Alossaimi MA, Elsawaf LA, Devanathadesikan Seshadri V, Almurshedi AS, et al. Central Composite Optimization of Glycerosomes for the Enhanced Oral Bioavailability and Brain Delivery of Quetiapine Fumarate. Pharmaceuticals 2022; 15:940. https://doi.org/10.3390/ph15080940.
22. Alam MS, Sultana N, Rashid MA, Alhamhoom Y, Ali A, Waheed A, et al. Quality by Design-Optimized Glycerosome-Enabled Nanosunscreen Gel of Rutin Hydrate. Gels 2023; 9:752. https://doi.org/10.3390/gels9090752.
23. Alkefai NH. Microneedle-Assisted Delivery of Berberine-Loaded Glycerosomes: a Novel Strategy for Psoriasis Treatment. J Clust Sci 2026; 37:13. https://doi.org/10.1007/s10876-025-02971-3.
24. Md S, Alhakamy NA, Aldawsari HM, Husain M, Khan N, Alfaleh MA, et al. Plumbagin-Loaded Glycerosome Gel as Topical Delivery System for Skin Cancer Therapy. Polymers 2021;13:923. https://doi.org/10.3390/polym13060923.
25. Zhang K, Zhang Y, Li Z, Li N, Feng N. Essential oil-mediated glycerosomes increase transdermal paeoniflorin delivery: optimization, characterization, and evaluation in vitro and in vivo. Int J Nanomedicine 2017; 12:3521–32. https://doi.org/10.2147/IJN.S135749.
26. Khan MA, Naseer MA, Rani D, Chauhan B, Ali Z. Formulation and development of griseofulvin-loaded glycerosomal nanogel for the management of onychomycosis. Drug Discov Dev 2026:1–11. https://doi.org/10.5530/ddd.2.2.9.
27. Mohamed Abd El-Emamed M, Ibrahim M, Qelliny MR, Mostafa M, El Sayed MM, Kilany MS, et al. Rosuvastatin-Loaded Glycerosomes as a Neuroprotective Strategy Against Hyperlipidemia-Induced Brain Dysfunction: Development, Optimization, and in vivo Evaluation. J Pharm Innov 2026; 21:160. https://doi.org/10.1007/s12247-025-10286-z.
28. Sharma N, Mazumder R, Rai P, Debnath A. Digoxin as a PD-1 Inhibitor: In Silico Analysis, NMR Characterization, Cytotoxicity Evaluation, and Glycerosome-Mediated Delivery for Enhanced Skin Cancer Therapy. J Pharm Innov 2026;21:155. https://doi.org/10.1007/s12247-026-10390-8.

29. Safiul Fitria NI, Erawati T, Miatmoko A, Soeratri W. Characterization and Stability Test of Hydrolyzed Collagen Glyserosomes 2024.
30. Sayyed ME, Hatem S. Glycerol-based soft vesicular systems for nose to brain delivery of 131I-melatonin: Synthesis, characterization, biodistribution and Pharmacokinetic investigations. J Drug Deliv Sci Technol 2025; 114:107482. https://doi.org/10.1016/j.jddst.2025.107482.
31. Johl S, Bhattacharyya S. Novel Deformable Vesicle for the Transdermal Delivery of Terbinafine Hydrochloride-Formulation and Cytotoxic Evaluation. Indian J Pharm Educ Res 2024; 58:460–9. https://doi.org/10.5530/ijper.58.2.52.
32. AbouSamra MM, Farouk F, Abdelhamed FM, Emam KAF, Abdeltawab NF, Salama AH. Synergistic approach for acne vulgaris treatment using glycerosomes loaded with lincomycin and lauric acid: Formulation, in silico, in vitro, LC-MS/MS skin deposition assay and in vivo evaluation. Int J Pharm 2023; 646:123487. https://doi.org/10.1016/j.ijpharm.2023.123487.
33. Magdy M, Elmowafy E, Elassal M, Ishak RAH. Glycerospanlastics: State-of-the-art two-in-one nano-vesicles for boosting ear drug delivery in otitis media treatment. Int J Pharm 2023; 645:123406. https://doi.org/10.1016/j.ijpharm.2023.123406.
34. [34] Siddique W, Zaman M, Waheed S, Sarfraz RM, Bashir S, Minhas MU, et al. Development and optimization of ganciclovir-loaded carbopol topical gel by response surface methodology for enhanced skin permeation. Polym Bull 2023;80:11817–44. https://doi.org/10.1007/s00289-022-04612-5.
35. Imam SS, Gilani SJ, Zafar A, Jumah MNB, Alshehri S. Formulation of Miconazole-Loaded Chitosan–Carbopol Vesicular Gel: Optimization to In Vitro Characterization, Irritation, and Antifungal Assessment. Pharmaceutics 2023;15:581. https://doi.org/10.3390/pharmaceutics15020581.
36. Pahlevi MR, Maulida IH, Supriadi D, Pratama R. Formulation of Moringa Leaf Ethanol Extract Gel (Moringa oleifera L.) Using Carbopol 940 as a Gelling Agent and Antioxidant Activity. Trop J Nat Prod Res 2026;10:7284. https://doi.org/10.26538/tjnpr/v10i2.36.
37. Ozon EA, Anastasescu M, Musuc AM, Burloiu AM, Socoteanu RP, Atkinson I, et al. Formulation and Characterization of Carbopol-Based Porphyrin Gels for Targeted Dermato-Oncological Therapy: Physicochemical and Pharmacotechnical Insights. Int J Mol Sci 2025;26:3641. https://doi.org/10.3390/ijms26083641.
38. Ojha C, Sharma P, Jain V. Design, optimization, and evaluation of topical gel of Cardiospermum halicacabum and Ricinus communis L. leaves extract for the treatment of rheumatoid arthritis. J Biomater Sci Polym Ed 2024; 35:1584–605. https://doi.org/10.1080/09205063.2024.2340872.
39. Ghazwani M, Hani U, Alam A, Alqarni MH. Quality-by-Design-Assisted Optimization of Carvacrol Oil-Loaded Niosomal Gel for Anti-Inflammatory Efficacy by Topical Route. Gels 2023; 9:401. https://doi.org/10.3390/gels9050401.
40. Abdelfattah S, Mady FM, Sarhan HA, Khalifa HO, Hashem H, Hassan H, et al. Topical delivery of meropenem via spanlastic carbopol gel: in-vitro studies and in-vivo application in pressure ulcers. Front Pharmacol 2025; 16:1672677. https://doi.org/10.3389/fphar.2025.1672677.
41. Elhabal SF, Mahfouz OM, Elrefai MFM, Teaima MH, kholeif N ahmed, El-Nabarawi M. Innovative chitosan-based microneedle patch for sustained ocular delivery of bisoprolol-loaded glycerosomes: *In vitro* and *in vivo* efficacy for treating glaucoma. J Drug Deliv Sci Technol 2026; 122:108379. https://doi.org/10.1016/j.jddst.2026.108379.
42. Afzal H, Taj MB, Alsabban MM, Alelwani W, Alahmadi N, Zaidi N, et al. Design of chitosan-coated CeO2-doped ZnCr LDO nanocomposites for optimized azithromycin delivery: a kinetic and mechanistic perspective. RSC Med Chem 2025; 16:4742–66. https://doi.org/10.1039/D5MD00455A.
43. Yu J, Zheng M. Application of Probabilitybasedmulti - Objective Optimizationinthe Preparation Of Drugencapsulation with A Designedexperiment. Mil Tech Cour Vojnoteh Glas 2022; 70:924. https://doi.org/10.5937/vojtehg70-38011.
44. Maan S, Khar RK, Mazumder R, Yadav N, Khan UA. Fabrication and Evaluation of Controlled Release Transdermal Drug Delivery System of Carvedilol using Design Expert® Software for the Management of Hypertension. J Young Pharm 2022; 14:295. https://doi.org/10.5530/jyp.2022.14.58.
45. Gómez-García F-J, Ramírez-Andreo A, Manconi M, Manca M-L, Matricardi P, di-Meo C, et al. In vitro and in vivo efficacy evaluation of new self-assembling curcumin loaded nanohyaluronan-glycerosomes on wound restoring in health and diabetic rats 2025. https://doi.org/10.1016/j.ijbiomac.2025.144699.
46. Belal M, Labib GS, Ghareeb DA, Helmy MW, El-Masry SM. Biofriendly resveratrol loaded glycerosomal nanovesicles improve wound healing in chronic diabetic foot ulcers: *In-vitro* & *in-vivo* efficacy evaluation. J Drug Deliv Sci Technol 2024; 97:105805. https://doi.org/10.1016/j.jddst.2024.105805.
47. Mansour MF, Husseini RA, Abdo SA, Khamis T, Mohammed HA, Alsemeh AE, et al. Mechanistic insights into the lipotropic and atheroprotective effects of rosuvastatin-loaded glycerosomes in dyslipidemic rats. Sci Rep 2026; 16:4390. https://doi.org/10.1038/s41598-025-34918-z.
48. Kharbanda J, Mazumder R, Bhardwaj S, Mazumder A, Mishra R, Mishra R, et al. Phytoconstituents-Based Nanotherapeutic Approach for the Effective Management of Joint Inflammatory Condition: Arthritis. Curr Drug Targets 2024; 25:700–14. https://doi.org/10.2174/0113894501306516240531053653.
49. Fulgheri F, Angius F, Perra M, Delogu I, Puxeddu S, Georgiev MI, et al. Liposomal Delivery of a Biotechnological Lavandula angustifolia Miller Extract Rich in Rosmarinic Acid for Topical Herpes Simplex Therapy. Antioxidants 2025; 14:811. https://doi.org/10.3390/antiox14070811.